Understanding the performance degradation and recovery of passive direct ethanol fuel cell

Panuwat Ekdharmasuit[1,*]

[1]Faculty of Science, Energy and Environment, King Mongkut's University of Technology North Bangkok, Rayong Campus, Rayong, 21120, Thailand

Abstract. In developing a fuel cell, one of the major issues that obstruct the commercialization of fuel cells is cell degradation. Meanwhile, the recovery process is an important factor to upgrade the performance and durability of fuel cell system. In this work, a passive direct ethanol fuel cell (DEFC) recovered from the unused aged cell was investigated. The hydrogen evolution method was applied for recovering the cell performance. Electrochemical tools including cell polarization, anode polarization, electrochemical impedance spectroscopy (EIS), ethanol crossover measurement, and chronoamperometry were conducted to examine the activation phenomenon. The polarization curve of the fresh membrane electrode assembly (MEA) was obviously superior to the aged one. The maximum power density was decreased from 1.10 to 0.06 $mW \cdot cm^{-2}$ reaching an approximate 95% decrement after keeping the cell for 1 year. The polarization curve of the MEA after conducting hydrogen evolution was better than that before. The maximum power density was enhanced from 0.06 to 0.07 $mW \cdot cm^{-2}$ presenting an approximate 16.67% increment after recovering the cell. The MEA after the recovery process could reduce ohmic resistance by 67.40% indicating the enhancement of ionic and electronic conductivity and could improve kinetic reaction at the electrode. In conclusion, the recovery process would be helpful for the unused aged cell to improve the performance shortly.

Keyword. Direct ethanol fuel cell (DEFC), Passive fuel cell, Cell recovery process, hydrogen evolution method, Degradation

1 Introduction

Direct alcohol fuel cells (DLFCs) are devices that convert the chemical energy directly to electricity via a redox reaction of liquid fuel and oxidant. The advantages of DLFCs are simplicity, efficiency, low emissions, absence of moving parts and conveniently fuelling without a reforming step [1,2]. These make the DLFCs attractive to be a promising alternative power source for conventional batteries for portable devices.

Among all the investigated DLFCs, direct methanol fuel cells (DMFCs) are one of the most attention research due to the outstanding properties of methanol, such as high energy density, good electrochemical activity, biodegradable and relatively cheap [3]. It is notable that, to commercialize the DMFCs, the study of cell degradation behaviors is known to be another important issue. As we know, degradation behavior in a fuel cell is a combination of permanent and temporary degradation. Permanent degradation originates from electrode materials that are irrecoverable, such as MEA structure degradation, catalyst particle agglomeration/dissolution, catalyst dissolution and crossover, membrane degradation, gas diffusion layers and bipolar plates degradation, etc. While, temporary degradation is based on operating conditions and some reversible materials changes, such as the cathode water flooding, CO_2 accumulation at the anode, Pt oxides formation, etc. and can be recovered either partially or fully.

As of now, researchers have explored the strategies to recover and boost up cell performance due to temporary degradation during the cell operation in a long-term test, which is called the performance recovery technique. Hydrogen evolution is one of the recovery techniques for upgrading DMFC performance. It was observed that, after hydrogen evolution, cell performance was improved due to the improved porosity and tortuosity of the catalyst layers [4] and the oxidative removal of methanol and other reaction intermediates at the catalyst and thereby reducing the catalyst surface oxides leading to a very stable voltage in a long-term test [5,6].

In comparison with DMFCs, the direct ethanol fuel cells (DEFCs) have been introduced to be another great potential for commercialization on account of their advantages of ethanol over other types of liquid fuel, such as high gravimetric energy density, non-toxicity, and availability from renewable sources [7]. Theoretically, protons, electrons and carbon dioxide are obtained at the anode from the ethanol oxidation reaction, while the water is produced at the cathode from the oxygen reduction reaction. In addition, the main products of ethanol oxidation could change to acetaldehyde, acetic acid,

* Corresponding author: panuwat.e@sciee.kmutnb.ac.th

carbon dioxide, protons and electrons in case of low temperature operating condition. The reactions are shown in equations (1)-(5) [8].

Ethanol oxidation:

$$C_2H_5OH + 3H_2O \rightarrow 2CO_2 + 12\,H^+ + 12e^- \quad (E^0_{anode} = 0.084\ V) \qquad (1)$$

Oxygen reduction:

$$3O_2 + 12H^+ + 12e^- \rightarrow 6H_2O \quad (E^0_{cathode} = 1.229\ V) \qquad (2)$$

Overall reaction:

$$C_2H_5OH + 3O_2 \rightarrow 2CO_2 + 3H_2O \quad (E^0_{cell} = 1.145\ V) \qquad (3)$$

Partial ethanol oxidation:

$$C_2H_5OH \rightarrow CH_3CHO + 2H^+ + 2e^- \qquad (4)$$

or

$$C_2H_5OH + H_2O \rightarrow CH_3COOH + 4H^+ + 4e^- \qquad (5)$$

Unfortunately, the kinetic reaction and liquid crossover behavior in DEFC would be different features compared to that in DMFC because of the higher molecular weight of ethanol and the slower kinetic rate of ethanol reaction on the Pt catalyst utilized at the cathode. Hence, it was expected that the impact of the activation procedure and the degradation mechanism of a DEFC would be different from its impact on a DMFC.

Recently, the degradation and recovery techniques are investigated in the DEFC during cell operation. Li *et al.* [9] conducted a 520-h long-term durability test of the alkaline DEFC and observed that the cell performance was degraded mainly due to the reduction of the electrochemical-active surface area at the anode. Jablonski *et al.* [10] introduced the periodic short circuit in the pulsed mode of the DEFC electrodes, which could increase both the OCV and efficiency of a DEFC operation due to the oxidation of CO and ethanol to CO_2 and afterward free the catalyst surface at the anode. In addition, the operating concept of DEFC can be classified into an active system requiring power for auxiliary parts and a passive system that involves no energy-consuming auxiliary device for the supply of reactants [8]. Passive DEFC exhibits different mass and heat transport patterns in comparison with active DEFC. The research on passive DEFC is rare and lacks sufficient information with respect to the exact changes, which occur in the MEA recovery behavior. Moreover, in the case of aged MEA of a fuel cell, the performance loss occurs due to cell degradation of both permanent and temporary features. The recovery techniques would be important in realizing a cell performance improvement from the temporary degradation.

In this work, as an attempt at passive DEFC recovery from the unused aged cell, we applied the hydrogen evolution method for recovering the cell performance. Electrochemical tools including cell polarization, anode polarization, electrochemical impedance spectroscopy (EIS), ethanol crossover measurement, and chronoamperometry were conducted to investigate the cell degradation and activation phenomenon.

2 Materials and methods

2.1. Materials and cell fabrication

Nafion® 115 (Dupont) was used as a membrane in this work and prepared by three main steps consisting of cleaning in 3% H_2O_2 solution, boiling in 0.5 M H_2SO_4 solution, and washing in de-ionized water with the condition of 70°C for 1h at each process. The anode catalyst was Pt-Sn (3:1 a/o) on Vulcan XC72 carbon (Johnson Matthey), while the cathode was the commercial gas diffusion electrode (GDE, E-TEK Somerset NJ, USA) containing 0.5 mgPt·cm^{-2} on Vulcan XC72 carbon.

To prepare the anode catalyst ink solution, the anode catalyst powder, Nafion ionomer solution (5wt% in alcohol/water), and isopropyl alcohol were mixed with the aid of an ultrasonic bath for 1 h. The 5 cm^2 anode catalyst layer was prepared by painting the catalyst ink on the commercial gas diffusion layer (E-LAT®, E-TEK) and dried in an oven at 80°C for 1 h. The obtained anode catalyst layer had a metal loading of 2 mg·cm^{-2} with the Nafion ionomer loading of 20% of the dry catalyst layer. The anode and the cathode were fabricated onto each side of the Nafion membrane to construct the membrane electrode assemblys (MEAs) and then were inserted into the in-house fuel cell stack by compressing between two acrylic blocks as shown in Figure 1.

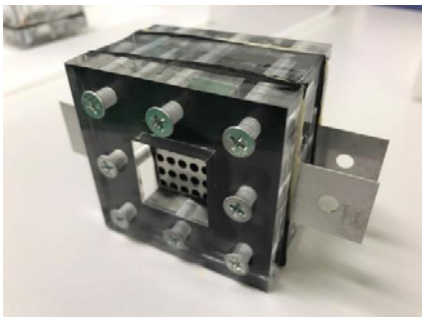

Figure 1. In-house fuel cell stack.

2.2. Cell performance test and electrochemical measurements

The performance and characterization results were obtained with a potentiostat/galvanostat apparatus (Metrohm Autolab, PGSTAT 302N, Utrecht, The Netherlands). The diagram of the apparatus set-up is shown in Figure 2.

Before cell testing, to obtain a steady-state cell behavior, a single cell was activated for 2 h by flowing ethanol solution at 1 M and 1 ml·min^{-1} at the anode and using ambient air, room temperature, atmospheric pressure, at the cathode. Thereafter, the single fresh cell

performance was tested by storing an ethanol concentration of 1 M at the anode and contacting with ambient air, room temperature, and atmospheric pressure, at the cathode. Then, the cell was kept in the box for 1 year without any cell operations (unused aged cell). After that, the cell was performed to investigate the performance change. In the beginning, the ethanol/air activation process was applied for 2 h to obtain a steady-state cell behavior with 1 M ethanol concentration, 1 ml·min^{-1} ethanol flow rate, at the anode and ambient air at room temperature, atmospheric pressure, at the cathode. Before H_2 evolution, cell characterizations were analyzed in a passive mode with 1 M ethanol concentration at the anode and ambient air at room temperature, and atmospheric pressure, at the cathode, using potentiostat/galvanostat. Whole cell polarization was measured by a potentiodynamic polarization mode from open circuit voltage (OCV) down to 0.1 V at a scan rate of 10 mV·s^{-1} and the time interval was set as 10 seconds per point. The anode polarization measurement was performed in a potentiodynamic polarization mode at a scan rate of 10 mV·s^{-1} by storing ethanol solution at the anode side and supplying unhumidified hydrogen gas to the cathode at a flow rate of 100 mL·min^{-1} as a dynamic hydrogen electrode (DHE). The protons generated in the anode due to the ethanol oxidation reaction migrated to the cathode and reduced, thereby delivering the hydrogen gas that acted as DHE [11].

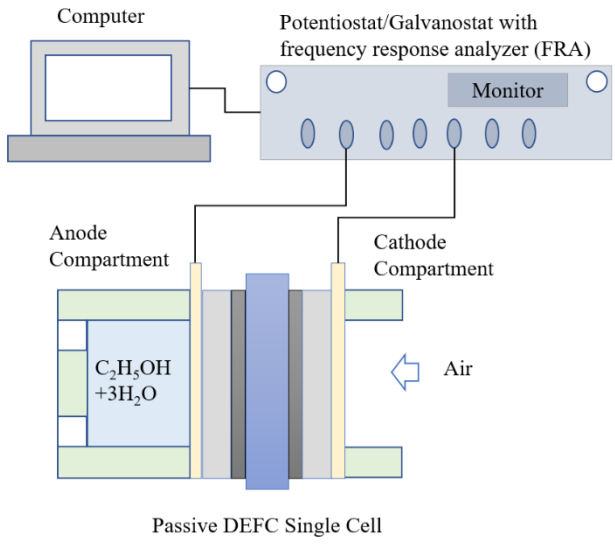

Figure 2. A schematic diagram of apparatus set-up.

EIS measurement was recorded in potentiostatic mode at 0.2 V and the measured frequency was ranged from 5 kHz to 0.05 Hz with 10 points per decade and the amplitude of 20 mV. In the case of the whole cell, impedance spectra were carried out by storing ethanol solution at the anode as a working electrode (WE) and opening to natural air at the cathode as reference (RE) and counter electrode (CE), while the anode impedance spectra were conducted by storing ethanol solution at the anode as a working electrode (WE) and hydrogen gas at the cathode at a flow rate of 100 mL·min^{-1} as a DHE. Further, ethanol crossover by the voltammetric method was conducted by taking purity nitrogen gas (99.98%) to the cathode at a flow rate of 100 mL·min^{-1} as WE and the ethanol solution of 1 M to the anode in passive mode as RE and CE. The applied voltage was varied from 0 to 1.2 V at a scan rate of 2 mV·s^{-1}. The reaction at the anode is hydrogen evolution, while the reaction at the cathode is the oxidation of ethanol crossed from the anode to the cathode [12]. The current discharging with time (chronoamperometry) at the voltage of 0.3 V for 20 min was conducted to investigate the performance behavior during steady state condition.

2.3. Recovery method

The hydrogen evolution technique at the cathode was conducted to recover the cell performance following the procedure elsewhere [6]. Ethanol solution with a concentration of 1.0 M at 1.0 ml·min^{-1} was fed to the anode, while N_2 gas was supplied to the cathode at 100 sccm. The anode was connected with the positive terminal of a and the cathode was connected with the negative terminal. This technique was controlled at a current density of 0.3 V for 10 min. The ethanol was oxidized at the anode to generate protons, electrons, and other products. Protons and electrons moved to the cathode and then they recombined to generate hydrogen. A schematic diagram explaining the hydrogen evolution process at the cathode is presented in Figure 3. Also, The hydrogen evolution at the anode was performed. It was the reverse of the previous procedure at the cathode. For comparison, cell characterizations were analyzed again after hydrogen evolution using the same procedure as conducted before activation.

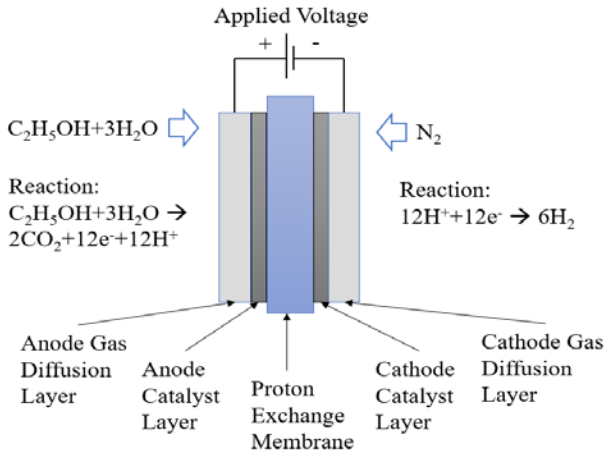

Figure 3. A schematic representation of the H_2 evolution process at the DEFC cathode.

3 Results and discussions

3.1. Cell performance degradation

At the beginning, single fresh cell performance was tested with an ethanol concentration of 1 M at the anode and fed

with ambient air, room temperature, and atmospheric pressure, at the cathode. After that, the cell was kept in the box for 1 year without any cell operations (unused aged cell). The performance of the unused aged cell was tested and compared to that of the fresh cell. Figure 4 shows the comparison of the polarization and power density curves of the fresh and aged MEA. The polarization curve of the fresh MEA was much better than that of the aged one. The maximum power density is decreased from 1.10 to 0.06 $mW \cdot cm^{-2}$ reaching an approximate 95% decrement after keeping the cell for 1 year, corresponding to the degradation rate of around 1.19 x 10^{-4} $mW \cdot cm^{-2}/h$. The degradation rate in this case is different compared with that in aged DEFC in continuous operation of 500 h (0.03 $mW \cdot cm^{-2}/h$) [9], in aged DMFC in continuous testing of 4044 h (6.18 x 10^{-3} $mW \cdot cm^{-2}/h$) [13] and in aged passive DMFC in continuous operation of 3000 h (3.33 x 10^{-3} to 4.33 $mW \cdot cm^{-2}/h$) [14].

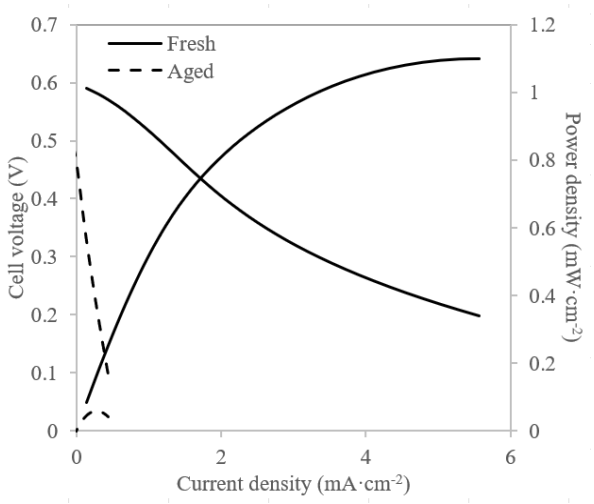

Figure 4. Influence of cell degradation on the cell performance curve.

To better understand the resistance mechanism, the comparison of Nyquist plots by EIS for the MEA before and after hydrogen evolution was carried out, shown in Figure 5. The EIS data were obtained by considering the values at the x-axis intercept, which represented the cell ohmic resistance. The intersection of the fresh MEA takes place at the lower resistance value in the real axis in a comparison with that of the aged MEA. The resistance decreases from 0.4 ohms for the fresh MEA to 1.9 ohms for the aged MEA. This demonstrates that the fresh MEA had much lower ohmic resistance caused by the lower both ionic and electronic conductivity. Besides, the size of the semicircle regards the kinetics of ethanol oxidation. It was found that the size of the fresh MEA is much smaller than that of the aged MEA due to the lower kinetic resistance of the fresh MEA.

3.2. Cell performance after the recovery process

Consequently, as an attempt to recover the unused aged cell, the hydrogen evolution method was devoted to both the anode and cathode for recovering the cell performance. Figure 6 shows the comparison of the polarization and power density curves of MEA before and after the recovery process by hydrogen evolution at both electrodes. The polarization curve of the MEA after conducting hydrogen treatment is better than that before. The maximum power density was enhanced from 0.06 to 0.07 $mW \cdot cm^{-2}$ presenting an approximate 16.67% increment after hydrogen evolution, similar to that reported in Ref. [6], which was improved by an approximate 9.5 to 14.3%.

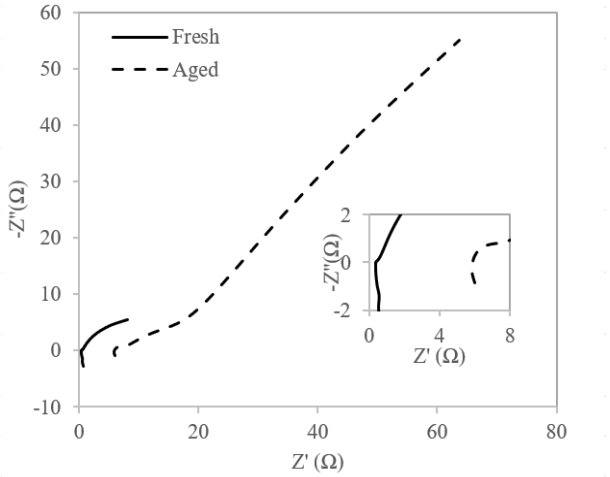

Figure 5. Influence of cell degradation on whole cell Nyquist plot.

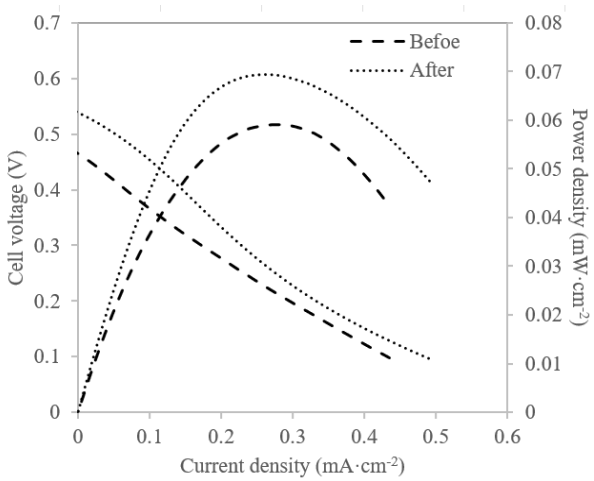

Figure 6. Influence of cell recovery on the cell performance curve.

Figure 7 shows the comparison of Nyquist plots for the MEA before and after the recovery process. The ohmic resistance value (the intersection value at high frequency) of the MEA before the recovery (approximately 5.89 ohms) was higher than that of the MEA after the cell recovery (approximately 1.92 ohms). The cell ohmic loss was reduced by 67.40% after applying the recovery process. This indicates that the MEA after the recovery could enhance cell ohmic resistance caused by the improvement of ionic and electronic conductivity. Moreover, it was observed that the size of the semicircle for the MEA after recovery tends to be smaller than that

of the MEA before the recovery due to the lower kinetic resistance of the MEA after the recovery process.

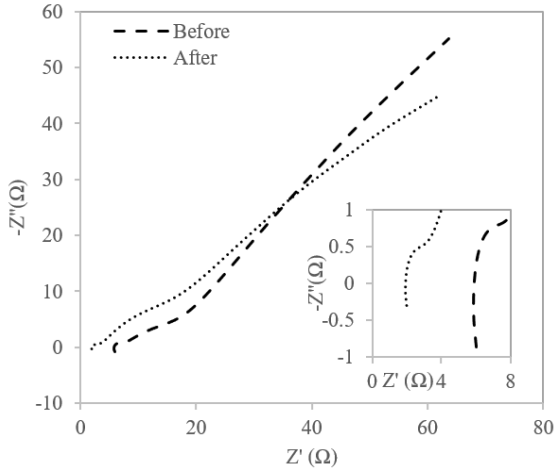

Figure 7. Influence of cell recovery on whole cell Nyquist plot.

Figure 8 shows the comparison of the anode potentials of MEA before and after the recovery process. The result shows that the current of MEA after the recovery process was higher than that of MEA before recovery throughout the voltage range. The current density at the high voltage region of around 0.6 V versus DHE was considered the anode-limiting current density. The MEA after recovery had the anode limiting current density of 1.13 mA·cm^{-2}, which was 10.78% higher than that of MEA before recovery (1.02 mA·cm^{-2}). This can explain that the recovery process could upgrade both the anode kinetic of ethanol oxidation and mass transfer resistance.

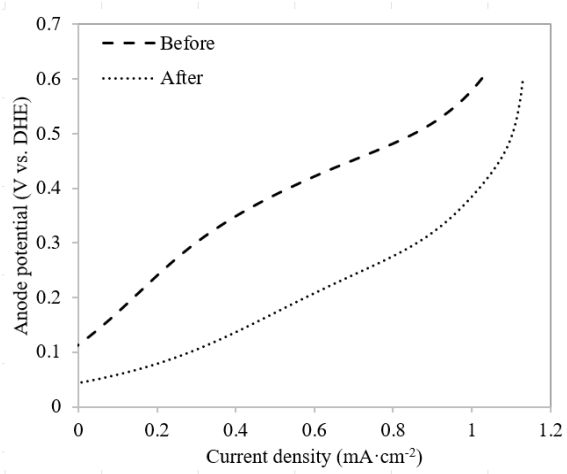

Figure 8. Influence of cell recovery on anode current density.

Figure 9 shows the comparison of Nyquist plots for the anode of MEA before and after the recovery process. The intersection of the MEA before the recovery takes place at the higher resistance value in the real axis in a comparison with that of the MEA after the recovery. The anode ohmic resistance value of the MEA before the recovery (5.27 ohms) is much higher than that of the MEA after the cell recovery (2.58 ohms). It is seen that the ohmic loss at the anode electrode could be reduced by 51.04% after conducting the recovery process. Apparently, it is found that the ohmic loss was mainly reduced at the anode leading to the improvement of cell performance. It should also be mentioned that the order of the resistance observed in the anode half cell is quite consistent with the cell resistance in the whole cell.

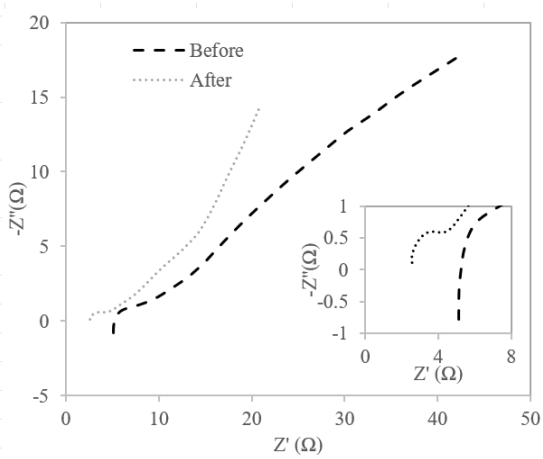

Figure 9. Influence of cell recovery on anode Nyquist plot.

In addition, the size of the semi-circle represents the charge transfer resistances of the cell. Therefore, the charge transfer resistances of the MEA after the recovery seems to be smaller than that of the MEA before the recovery. This result indicates that the recovery process could enhance the electrochemical reactions on the anode electrode.

Figure 10 shows the ethanol crossover current density versus the applied voltage of MEA before and after the recovery process. The current density was considered as the amounts of ethanol permeated from the anode to the cathode. The highest value of current density and a so-call peak crossover current density at the highest voltage was selected for the comparison. A peak crossover current density of MEA before the recovery process was 0.66 mA·cm^{-2}, which was lower than that of MEA after the recovery process at 1.44 mA·cm^{-2}. This means that the MEA after the recovery process increased the crossover of ethanol solution through the membrane. It might be explained that the membrane is completely saturated during the recovery process promoting ethanol diffusivity across the membrane.

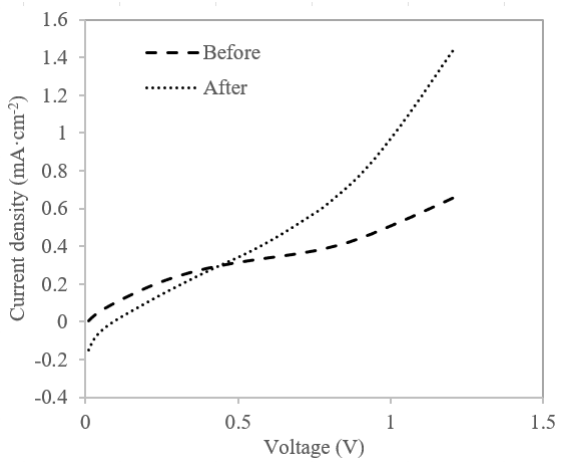

Figure 10. Influence of cell recovery on ethanol crossover current density.

Figure 11 shows the current discharging with time at the voltage of 0.3 V. The result shows that the current of MEA after the recovery process was higher than that of MEA before recovery for the entire time. Moreover, the signal of current discharging of MEA after the recovery process was obviously stable and uniform. It is believed that the MEA after the recovery process could effectively reduce the catalyst surface oxides and maintain a stable current density during cell operation [6].

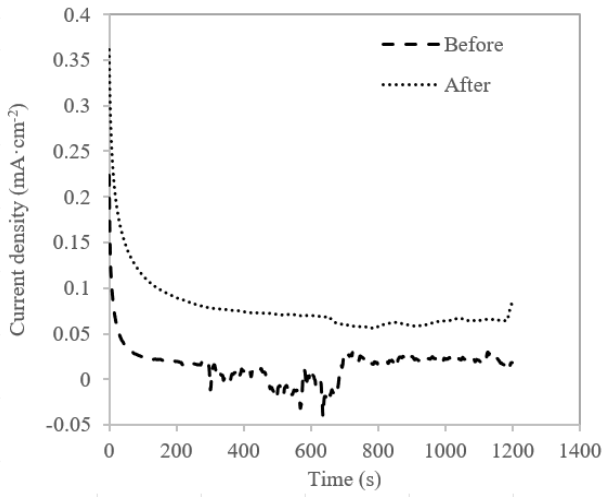

Figure 11. Influence of cell recovery on cell current density variation with time for 20 min.

4 Conclusions

A passive DEFC recovery from the unused aged cell was investigated. The hydrogen evolution method was performed to recover the cell performance. The polarization curve of the fresh MEA was obviously superior to the aged one. The maximum power density was decreased from 1.10 to 0.06 $mW \cdot cm^{-2}$ reaching an approximate 95% decrement after keeping the cell for 1 year. The loss of cell performance was mainly for both the ohmic and the kinetic resistance. Consequently, the cell was recovered by the hydrogen treatment process.

The performance of the MEA after conducting the recovery was improved. The maximum power density was enhanced from 0.06 to 0.07 $mW \cdot cm^{-2}$ presenting an approximate 16.67% increment after recovering the cell. The cell ohmic loss was reduced by 67.40% after applying the recovery process and the kinetic reaction was improved at the electrode. At the anode, the ohmic loss and kinetic activation loss could be reduced after conducting the recovery process. It can be seen that the ohmic loss was mainly reduced at the anode. Also, the crossover of ethanol solution through the membrane was improved after the activation due to the complete saturation in the membrane during the recovery process promoting ethanol diffusivity across the membrane.

Finally, the current discharging with time at the voltage indicated that the MEA after the recovery process could effectively reduce the catalyst surface oxides leading to a stable current density during cell operation. In conclusion, the recovery process would be helpful for the unused aged cell to improve the performance effectively and shortly.

Acknowledgements

This research was funded by King Mongkut's University of Technology North Bangkok [Contract no. KMUTNB-61-DRIVE-030] and the author would like to acknowledge the facility supported from Faculty of Science, Energy and Environment (SCIEE), King Mongkut's University of Technology North Bangkok, Rayong Campus.

References

1. J. Wang, Barriers of scaling-up fuel cells: Cost, durability and reliability, Energy, 80 (2015): 509-521
2. J.P. Pereira, D.S. Falcao, V.B. Oliveira, and A.M.F.R. Pinto, Performance of a passive direct ethanol fuel cell, Journal of Power Sources, 256 (2014): 14-19
3. C. Lamy, A. Lima, V. LeRhun, F. Delime, et al., Recent advances in the development of direct alcohol fuel cells (DAFC), Journal of Power Sources, 105 (2002): 283-296
4. Q. Ye, T.S. Zhao, Electrolytic Hydrogen Evolution in DMFCs Induced by Oxygen Interruptions and Its Effect on Cell Performance, Electrochemical and Solid-state Letters, 8(4) (2005): A211-A214
5. J. Prabhuram, T.S. Zhao, H. Yang, Methanol adsorbates on the DMFC cathode and their effect on the cell performance, Journal of Electroanalytical Chemistry, 578 (2005): 105-112
6. A. Mehmood, H.Y. Ha, Performance restoration of direct methanol fuel cells in long-term operation using a hydrogen evolution method, Applied Energy, 114 (2014): 164-171
7. L. An, T.S. Zhao, Y.S. Li, Carbon-neutral sustainable energy technology: Direct ethanol fuel cells, Renewable and Sustainable Energy Reviews, 50 (2015): 1462-1468
8. V.B. Oliveira, J.P. Pereira, A.M.F.R. Pinto, Modeling of passive direct ethanol fuel cells, Energy, 133 (2017): 652-665
9. Y.S. Li and T.S. Zhao, Understanding the performance degradation of anion-exchange membrane direct ethanol fuel cells, International Journal of Hydrogen Energy, 37, (2012): 4413-4421
10. A. Jablonski and A. Lewera, Improving the efficiency of a direct ethanol fuel cell by a periodic load change, Chinese Journal of Catalysis, 36, (2015): 496-501
11. J. Prabhuram, N.N. Krishnan, B. Choi, T.H. Lim, H.Y. Ha, S.K. Kim, Long-term durability test for direct methanol fuel cell made of hydrocarbon membrane, International Journal of Hydrogen Energy, 35 (2010): 6924-6933
12. S. Song, G. Wang, W. Zhou, X. Zhao, G. Sun, Q. Xin, et al., The effect of the MEA preparation procedure on both ethanol crossover and DEFC performance, Journal of Power Sources, 140 (2005): 103-110

13. F. Jing, R. Sun, S. Wang, H. Sun and G. Sun, Effect of the anode structure on the stability of direct methanol fuel cell, Energy Fuels, 34 (2020): 3850-3857

14. A.M. Zainoodin, S.K. Damarudin, M.S. Masdar, WR.W. Daud, A.B. Mohamad and J. Sahari, Investigation of MEA degradation in a passive direct methanol fuel cell under different modes of operation, Applied Energy, 135 (2014): 364-372